Journal of Molecular Catalysis A: Chemical 353–354 (2012) 215–219

Contents lists available at SciVerse ScienceDirect

Journal of Molecular Catalysis A: Chemical

journal homepage: www.elsevier.com/locate/molcata

Preparation of Mn_2O_3/SBA-15 catalyst with high loading and catalytic peroxidation for degradation of organic pollutants

Fenglei Cao, Hu Li, Zhenmin Xu, Jia Zhang, Ya Zhang, Yuning Huo*

The Education Ministry Key Lab of Resource Chemistry, Shanghai Key Laboratory of Rare Earth Functional Materials, Shanghai Normal University, Shanghai 200234, China

ARTICLE INFO

Article history:
Received 16 September 2011
Received in revised form
29 November 2011
Accepted 29 November 2011
Available online 8 December 2011

Keywords:
Mn_2O_3/SBA-15
NH_3/H_2O vapor-induced internal hydrolysis
Catalytic peroxidation
Methylene blue
Ethanol

ABSTRACT

Mn_2O_3 catalyst homogenously coated on the mesopore wall of SBA-15 had been successfully prepared via NH_3/H_2O vapor-induced internal hydrolysis process. The high Mn_2O_3 loading (up to 60 wt%) was efficiently obtained without pore blockage. According to the catalytic peroxidation reaction for degrading both methylene blue and ethanol at 30 °C with pH value of 7.0, Mn_2O_3/SBA-15 catalyst displayed the excellent catalytic activities owing to the well distribution of Mn_2O_3 with large specific surface area, indicative of the potential practical application. Additionally, the degradation yield could be improved via declining the pH value or increasing reaction temperature.

1. Introduction

Manganese oxides have presented considerable importance in many applications, such as ion-exchange, molecular adsorption, catalysis, electrochemistry and magnetism, due to the structural flexibility with novel chemical and physical properties [1,2]. For instance, Mn_2O_3 is a well-known catalyst owing to the advantages of cheapness and environment-friendly property. Mn_2O_3 has been found to be active and reusable for decomposing H_2O_2 into hydroxyl radical (•OH) during catalytic peroxidation of organic effluents with low concentration of organic compounds [3,4], besides the application for CO and NO_x removal from waste gas [5,6]. Therefore, limitation existed in traditional homogeneous Fenton reagent (comprising homogenous Fe^{2+} and H_2O_2) for catalytic peroxidation can be avoided, including the formation of iron-containing waste sludge, the irreversible loss of reagent and the low pH range (2.0–5.0) [7–9].

As we known, the homogenous distribution of metal oxides on the substrate with high specific surface area, such as mesoporous silica materials, is an effective route to achieve the high catalytic activity. However, the pore blockage of mesoporous materials at high loading of metal oxides is still difficult to solve [10,11], restricting the improvement of catalytic activity. Herein, we report the Mn_2O_3 catalyst homogenously coated on the wall of mesoporous SBA-15 via the NH_3/H_2O vapor-induced internal hydrolysis (VIH) method reported by Ogura et al. [12]. The high loading of Mn_2O_3 (up to 60 wt%) can be efficiently obtained without pore blockage. Additionally, Mn_2O_3/SBA-15 catalyst displayed the excellent catalytic peroxidation properties for degrading both methylene blue (MB) and ethanol in a wide pH range at low temperature.

2. Experimental

2.1. Catalyst preparation

All source chemicals (analytical grade) were purchased from Shanghai Chemical Regents Company and used without further purification. SBA-15 was synthesized according to previous reports [13]. In a typical preparation procedure of VIH method (Scheme 1), 10 mL 1.28×10^{-2} mol/L $Mn(Ac)_2{\cdot}2H_2O$ solution was impregnated into mesopores of 1.0 g SBA-15 with stirring at 60 °C until dryness. After multi-stepped impregnation with 10 wt% Mn_2O_3 (ratio of Mn_2O_3 to SBA-15) for each step, the precursor was heated at 100 °C for 6 h and the obtained solid materials were put into a 10 mL glass tube, which was located in one 50 mL Teflon autoclave containing 10.0 mL 14% $NH_3{\cdot}H_2O$. The tightly closed autoclave was heated to 60 °C for 4 h, followed by drying product at room temperature for 6 h and then at 100 °C for 12 h. Finally, the sample was calcined at 600 °C for 6 h to improve the crystallization and remove the residues. The as-prepared samples were denoted as X%Mn_2O_3/SBA-15, where X referred to the percentage of Mn_2O_3 loading.

* Corresponding author. Fax: +86 21 64322272.
E-mail address: Huoyuning@shnu.edu.cn (Y. Huo).

1381-1169/$ – see front matter © 2011 Elsevier B.V. All rights reserved.
doi:10.1016/j.molcata.2011.11.027

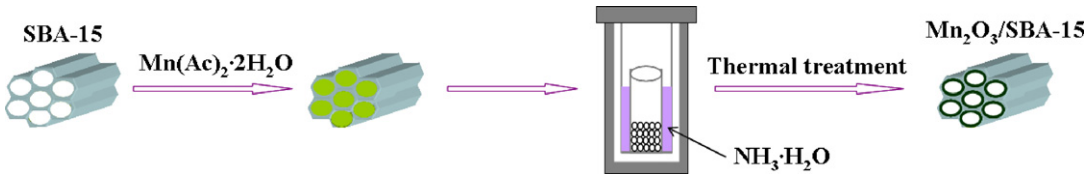

Scheme 1. Schematic illustration of preparation process.

2.2. Characterizations

The sample composition was determined by inductively coupled plasma (ICP, Varian VISTA-MPX). The catalyst structure was investigated by X-ray diffraction (XRD, Rigacu Dmax-3C, Cu Kα radiation). Surface morphology was observed through transmission electronic microscopy (TEM, JEM-2010). N_2 adsorption-desorption isotherms were measured on a Quantachrome NOVA 4000e at 77 K. The Brunauer–Emmett–Teller (BET) method was used to calculate the specific surface area (S_{BET}).

2.3. Activity test

Catalytic peroxidation reactions for the degradation of both MB and ethanol were used as the probe test to evaluate catalytic activity. The reaction system was carried out in a glass reactor connected to a condenser. 100 mL 15.0 mg/L MB or 50.0 mg/L ethanol solution containing 10.0 mg catalyst was stirred with the speed of 400 rpm. In order to exclude the absorption of catalysts for organics, catalysts were separated and added into another same solution after reaching absorption equilibrium for 1 h. Then, the catalytic peroxidation reaction was initiated by adding 0.5 mL H_2O_2 (30 wt%) at each interval of 30 min. Each run of reactions was lasted for 2 h and the total amount of H_2O_2 was 2.0 mL. The concentration of H_2O_2 was analyzed according to the previous report [14] and the amount of H_2O_2 was excess during the catalytic reactions. The pH value in the solution was adjusted via adding mixed solution of both 1.0×10^{-3} M HCl and 1.0×10^{-3} M NH_4Cl. After reaction for 2 h, the left MB was determined by UV spectrophotometer (UV 7504/PC) at the characteristic wavelength of 664 nm. Preliminary tests demonstrated a good linear relationship between the light absorbance and the compounds concentration. Meanwhile, the left ethanol was determined by the value of total organic carbon (TOC) measured on a Liqui Elementar. The degradation yield of organics was calculated by the following formula:

$$\text{Degradation yield}\,(\%) = \frac{C_0 - C}{C_0} \times 100$$

where C_0 and C referred to the concentration of MB or TOC value of ethanol before and after reaction, respectively. No obvious MB or ethanol degradation was observed after 2 h in the absence of catalyst, and only less than 10% MB or ethanol decomposed after reaction in the absence of H_2O_2, which could be neglected in comparison with the catalytic peroxidization process.

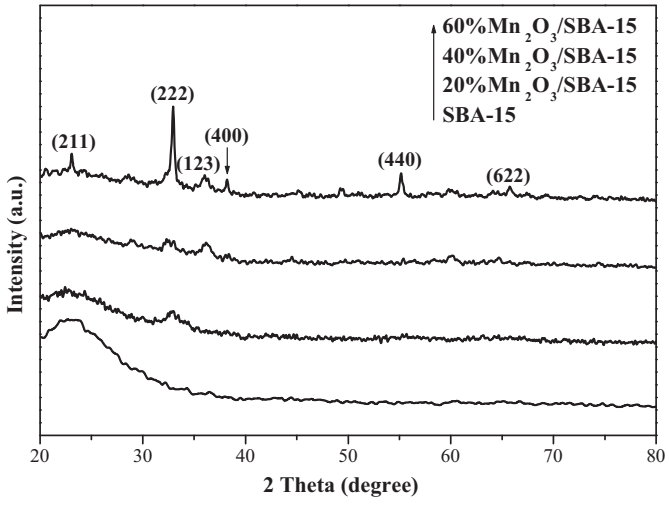

Fig. 1. Wide-angle XRD patterns of different samples.

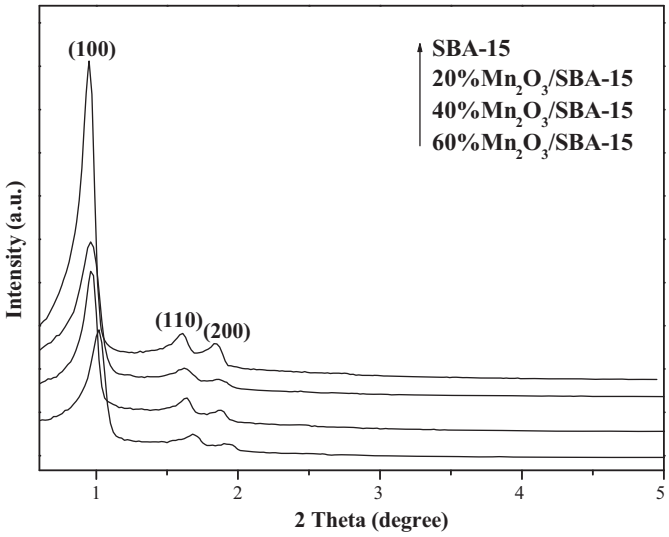

Fig. 2. Low-angle XRD patterns of different samples.

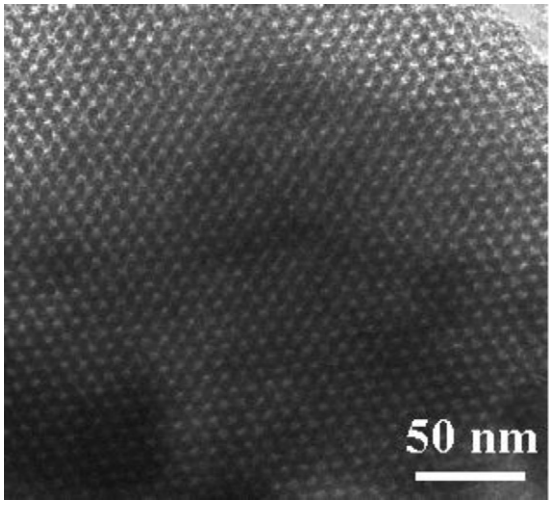

Fig. 3. TEM image of 40%Mn_2O_3/SBA-15.

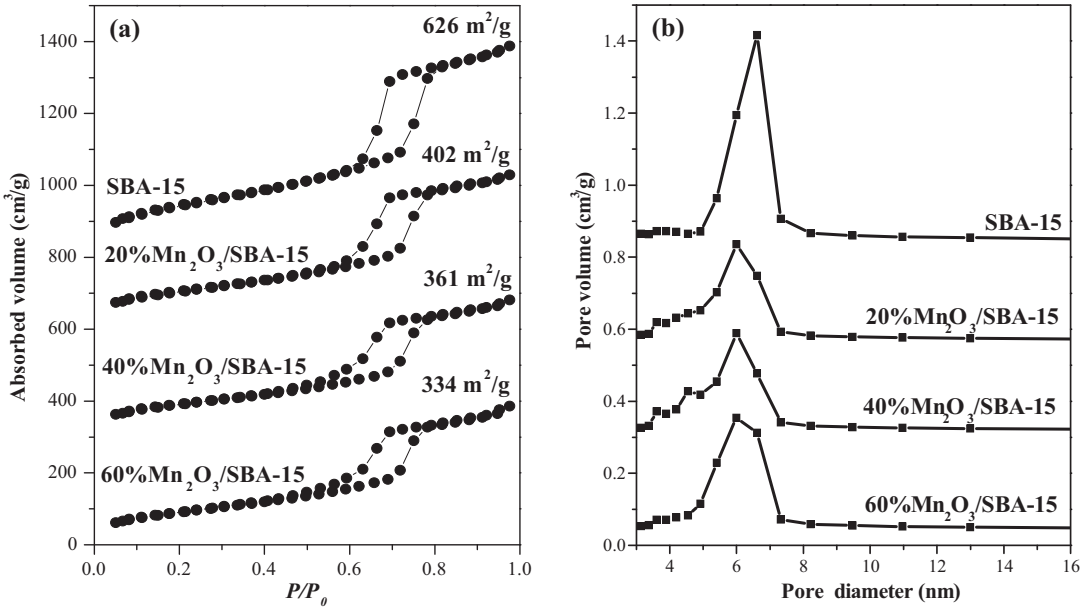

Fig. 4. (a) Nitrogen adsorption–desorption isotherms and (b) pore size distribution of different samples.

3. Results and discussion

ICP results demonstrated that the actual Mn_2O_3 content in $X\%Mn_2O_3$/SBA-15 catalysts was similar to the theory content. From Fig. 1, Wide-angle XRD patterns revealed that SBA-15 sample was amorphous and the crystallization of cubic Mn_2O_3 (JCPDS 78-0390) was enhanced with the increased loading of Mn_2O_3 in $X\%Mn_2O_3$/SBA-15 samples. However, the obvious diffraction peaks were only presented in $60\%Mn_2O_3$/SBA-15 after being calcined at 600 °C. It was suggested that Mn_2O_3 was mainly formed inside the mesopores of SBA-15 during the VIH process after the precursor filled the mesopores (Scheme 1), and thus the crystal growth of Mn_2O_3 was greatly inhibited. The presence of Mn_2O_3 crystal with low crystallization in $60\%Mn_2O_3$/SBA-15 was possibly owing to the slight amount of Mn_2O_3 particles existed outside of SBA-15 mesopores.

Low-angle XRD patterns of $X\%Mn_2O_3$/SBA-15 samples were shown in Fig. 2. SBA-15 exhibited three well-resolved peaks indexed as 100, 110 and 200 reflections, respectively, corresponding to the *p6mm* hexagonal symmetry in uniform 2D hexagonal pore structure [13]. More importantly, three diffraction peaks were also obviously presented in $X\%Mn_2O_3$/SBA-15 samples even at the highest Mn_2O_3 loading of 60 wt%, further confirming that the mesoporous structure in SBA-15 could be well maintained via the VIH process. It could be attributed that the Mn precursor was coordinated with NH_3 and then homogeneously distributed on the wall of SBA-15 mesopores under the high pressure of NH_3 vapor, preventing the blockage of mesopores and simultaneously achieving the uniform Mn_2O_3 coating within SBA-15 mesopores after calcination. The lower peak intensity in $X\%Mn_2O_3$/SBA-15 than that in SBA-15 could be resulted from the scatter of the X-rays by Mn_2O_3 catalyst rather than the collapse of pore structure [12]. The shift of peaks to the higher diffraction degree with the increased Mn_2O_3 loading in SBA-15 was due to the decreased diameter of mesopores. TEM image (Fig. 3) for $40\%Mn_2O_3$/SBA-15 sample exhibited the ordered

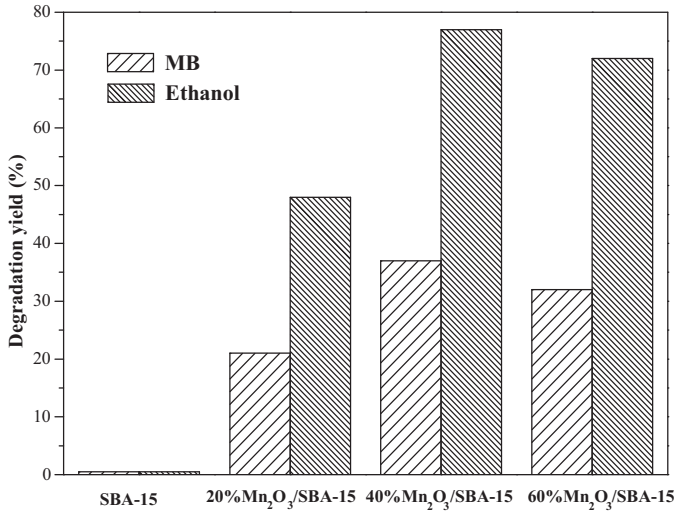

Fig. 5. Catalytic peroxidation activity for degrading MB and ethanol on different catalysts. Reaction conditions: 10.0 mg catalyst, 100 mL 15.0 mg/L MB or 50.0 mg/L ethanol solution, reaction time = 2 h, reaction temperature = 30 °C, pH = 7.0.

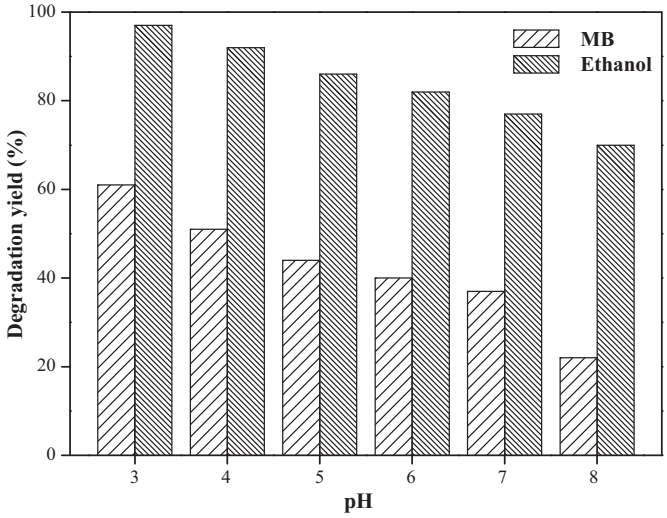

Fig. 6. Catalytic peroxidation activities of $40\%Mn_2O_3$/SBA-15 at different pH value. Reaction conditions: 10.0 mg catalyst, 100 mL 15.0 mg/L MB or 50.0 mg/L ethanol solution, reaction time = 2 h, reaction temperature = 30 °C.

mesopore structure without pore blockage, in accordance with the above XRD results.

The S_{BET} and porosity of $X\%Mn_2O_3$/SBA-15 samples were investigated via N_2 adsorption–desorption isotherm, as illustrated in Fig. 4. From Fig. 4(a), all of the isotherms could be categorized as type IV with the distinct hysteresis loop at about $p/p_o = 0.5–0.8$, indicative of the formation of mesoporous structure. All of $X\%Mn_2O_3$/SBA-15 samples revealed similar isotherms to SBA-15, resulting from the perfect maintenance of open mesopores without pore blockage even at the high Mn_2O_3 loading of 60 wt% [12]. With the increase of Mn_2O_3 loading, the volume of adsorbed nitrogen gradually decreased and the reduced hysteresis loop was shifted to a lower p/p_o value, corresponding to the decreased S_{BET}. Meanwhile, the wider pore size distribution and the smaller pore volume of $X\%Mn_2O_3$/SBA-15 samples than that of SBA-15 in Fig. 4(b) was also owing to the homogeneous Mn_2O_3 coating on the mesopore wall of SBA-15. The slightly decreased pore diameter of $X\%Mn_2O_3$/SBA-15 samples (about 6.0 nm) in comparison with SBA-15 could imply that Mn_2O_3 was coated as the uniform layer within SBA-15 mesopores rather than the nanocrystals [15].

The catalytic peroxidation for degrading both MB and ethanol, which were typical organic pollutants in the wastewater from dyeing industry and chemical industry, respectively, were used as a probe to evaluate the performances of different catalysts. According to Fig. 5, SBA-15 could not activate the degradation reaction, but all of $X\%Mn_2O_3$/SBA-15 samples exhibited the significant catalytic activity even when the pH was 7.0, demonstrating that Mn_2O_3 was the unique active site to decompose H_2O_2 into •OH radical and further oxide the organics, but SBA-15 only played the role of carrying and absorbing agent during the catalytic process. The highest yield of $40\%Mn_2O_3$/SBA-15 than other Mn_2O_3-loaded SBA-15 samples could be attributed that the well distribution of Mn_2O_3 in the SBA-15 mesopores and the maintained mesoporous structure after Mn_2O_3 loading, which could facilitate the efficient adsorption of organic molecular and generate the confinement effect to the organic molecules inside pores, improving the degradation of organics [16]. The extra loading led to the slight decline of degradation yield owing to the decreased S_{BET} and pore volume, which were unfavorable for the adsorption and transportation of organic molecular.

In addition, the effect of both pH value and reaction temperature to the degradation of organics was also investigated. From Fig. 6, the degradation yield of both MB and ethanol was gradually increased

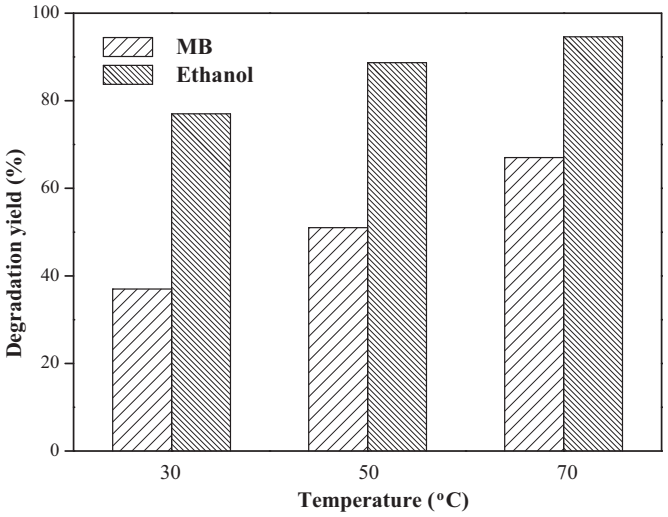

Fig. 7. Catalytic peroxidation activities of at elevated reaction temperature. Reaction conditions: 10.0 mg catalyst, 100 mL 15.0 mg/L MB or 50.0 mg/L ethanol solution, reaction time = 2 h, pH = 7.0.

with the decline of pH value, indicating that the acidic environment could promote the formation of •OH radical and thus facilitate the catalytic peroxidation process [16]. The decrease of yield from pH value of 3–8 was slow and could be accepted in the practical applications. In comparison with the conventional homogenous Fenton system only applicable in the pH range of 2.0–5.0, it was worth to consider the various advantages of Mn_2O_3/SBA-15 catalyst suitable for higher pH value, including the unnecessary addition of new compounds to adjust the pH value, the avoidance of extra treatment cost and the prevention of equipment corrosion. The catalytic peroxidation reaction could also be promoted by elevating the reaction temperature (Fig. 7). The increased yield at higher temperature was owing to the enhanced molecular diffusion and the more efficient utilization of active sites in catalyst. However, the reaction temperature of 30 °C was more suitable for the practical application, taking into account the acceptable decrease of yield and the energy consumption.

According to ICP result, it could be found that Mn_2O_3 was not decomposed after reaction since there was little Mn element which could be detected in the solution. Meanwhile, the

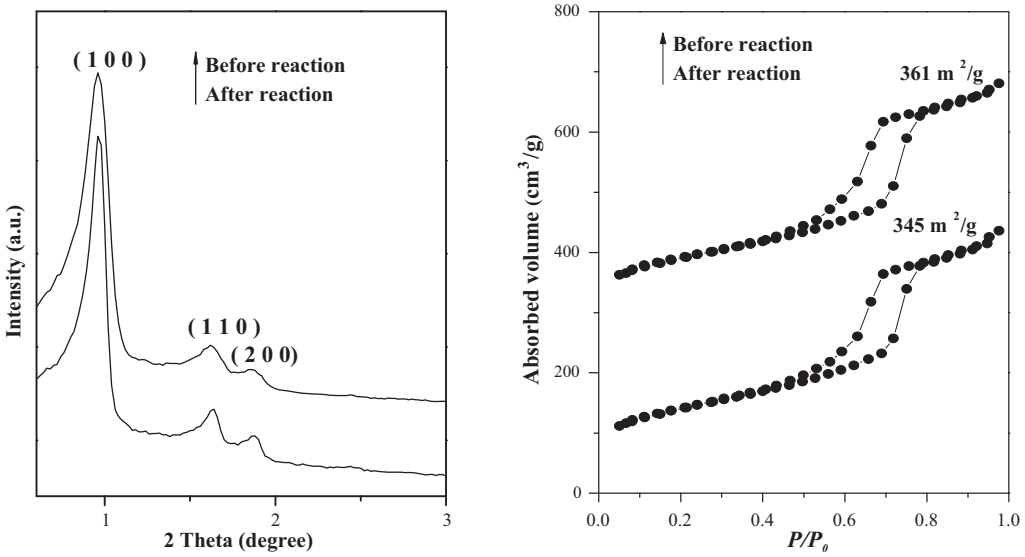

Fig. 8. Low-angle XRD patterns (left) and N_2 adsorption-desorption isotherms (right) of $40\%Mn_2O_3$/SBA-15 before and after reaction.

low-angle XRD patterns and N_2 adsorption–desorption isotherms of 40%Mn_2O_3/SBA-15 before and after reaction (Fig. 8) exhibited that the mesoporous structure was remained well after reaction. The slight decrease of S_{BET} was possible due to the organics existed on the catalyst, which could be easily removed by washing with deionized water. It could be resulted that Mn_2O_3 was stably existed within the pores of SBA-15 without pore blockage.

4. Conclusion

This work developed a facile approach to prepare Mn_2O_3/SBA-15 catalyst via NH_3/H_2O vapor-induced internal hydrolysis process. The Mn_2O_3 catalyst with high loading was demonstrated to be coated on the mesopore wall of SBA-15 without pore blockage. During the catalytic peroxidation activity for degrading both MB and ethanol even at 30 °C with pH value of 7.0, 40%Mn_2O_3/SBA-15 catalyst revealed the highest activity due to the well distribution of Mn_2O_3 with large specific surface area, implying the great potential in the future practical application. Meanwhile, both acidic environment and elevated temperature were favorable for the improvement of catalytic activity.

Acknowledgments

This work was supported by National Natural Science Foundation of China (20937003), Shanghai Government (11JC1409000, S30406, 12YZ091 and 10230711600) and Shanghai Normal University (DZL807 and SK201227).

References

[1] J. Fei, Y. Cui, X.H. Yan, W. Qi, Y. Yang, J.B. Li, Adv. Mater. 20 (2008) 452–456.
[2] W. Xiao, J.S. Chen, Q. Lu, X.W. Lou, J. Phys. Chem. C 114 (2010) 12048–12051.
[3] J.N. Park, J.K. Shon, M. Jin, S.H. Hwang, G.O. Park, J.H. Boo, T.H. Han, J.M. Kim, Chem. Lett. 39 (2010) 493–495.
[4] Y.N. Huo, Y. Zhang, Z.M. Xu, J. Zhu, H.X. Li, Res. Chem. Intermed. 35 (2009) 791–798.
[5] M. Baldi, V.S. Escribano, J.M.G. Amores, F. Milella, G. Busca, Appl. Catal. B 17 (1998) 175–182.
[6] H.M. Zhang, Y. Teraoka, N. Yamazoe, Catal. Today 6 (1989) 155–162.
[7] J.Y. Qin, Q. Zhang, K.T. Chuang, Appl. Catal. B 29 (2001) 115–123.
[8] H.Y. Chen, A. Sayari, A. Adnot, F. Larachi, Appl. Catal. B 32 (2001) 195–204.
[9] A.M.T. Silva, I.M. Castelo-Branco, R.M. Quinta-Ferreira, J. Levec, Chem. Eng. Sci. 58 (2003) 963–970.
[10] L. Vradman, M.V. Landau, M. Herskowitz, V. Ezersky, M. Talianker, S. Nikitenko, Y. Koltypin, A. Gedanken, J. Catal. 213 (2003) 163–175.
[11] L. Vradman, M.V. Landau, D. Kantorovich, Y. Koltypin, A. Gedanken, Micropor. Mesopor. Mater. 79 (2005) 307–318.
[12] C.K. Krishnan, T. Hayashi, M. Ogura, Adv. Mater. 9999 (2008) 1–6.
[13] D. Zhao, J. Feng, Q. Huo, N. Melosh, G.H. Fredrickson, B.F. Chmelka, G.D. Stucky, Science 279 (1998) 548–552.
[14] I.R. Cohen, T.C. Purcell, A.P. Altshuller, Environ. Sci. Technol. 1 (1967) 247–252.
[15] M.V. Landau, L. Vradman, X. Wang, L. Titleman, Micropor. Mesopor. Mater. 78 (2005) 117–129.
[16] Y.F. Han, F.X. Chen, K. Ramesh, Z.Y. Zhong, E. Widjaja, L.W. Chen, Appl. Catal. B 76 (2007) 227–234.